

MONA: Moving Object Detection from Videos Shot by Dynamic Camera

Boxun Hu^{*1}, Mingze Xia^{*1}, Ding Zhao¹, Guanlin Wu^{†1}

¹Johns Hopkins University

{bhu29, mxia8, dzhao29, gwu32}@jh.edu

^{*}Equal Contribution, [†]Corresponding Author

Abstract

Dynamic urban environments, characterized by moving cameras and objects, pose significant challenges for camera trajectory estimation by complicating the distinction between camera-induced and object motion. We introduce *MONA*, a novel framework designed for robust moving object detection and segmentation from videos shot by dynamic cameras. *MONA* comprises two key modules: *Dynamic Points Extraction*, which leverages optical flow and tracking any point to identify dynamic points, and *Moving Object Segmentation*, which employs adaptive bounding box filtering, and the Segment Anything for precise moving object segmentation. We validate *MONA* by integrating with the camera trajectory estimation method LEAP-VO, and it achieves state-of-the-art results on the MPI Sintel dataset comparing to existing methods. These results demonstrate *MONA*'s effectiveness for moving object detection and its potential in many other applications in the urban planning field.

Introduction

In recent years, advancements in artificial intelligence (AI) have spurred the development of innovative systems that are transforming urban environments. Notable examples include Autonomous Driving Systems (ADS) (Lang et al. 2019; Shi et al. 2019; Shi, Wang, and Li 2019) and low-altitude economy system (Huang et al. 2024; Li et al. 2024), which are reshaping urban mobility and infrastructure. Concurrently, sophisticated Human Motion Recovery (HMR) techniques (Ye et al. 2023; Shin et al. 2024; Shen et al. 2024) and human understanding methodologies (Chen et al. 2024a; Guo et al. 2022; Jiang et al. 2024) have enhanced the capabilities of human-AI collaboration in urban planning (Wang et al. 2019; Nikolakis, Maratos, and Makris 2019).

However, the complexity of urban scenarios poses significant challenges for existing methods in ADS (Shi et al. 2019; Lang et al. 2019), Unmanned Aerial Vehicle (UAV) motion planning (Zhou et al. 2021; Tordesillas and How 2023; Wu, Zhao, and He 2024), and HMR (Shin et al. 2024; Shen et al. 2024). These data-driven approaches often struggle to perform optimally across diverse and intricate real-world conditions. While increasing the volume of training data can enhance their performance by exposing models

to a broader range of scenarios, the acquisition of marker-based datasets—datasets with precise ground truth (GT) values—is prohibitively expensive. This limitation hampers the scalability and effectiveness of such methods.

Conversely, markerless datasets, which rely on pseudo-GT annotations generated through automated pipelines applied to vast quantities of online videos, offer a cost-effective alternative for augmenting training data (Lin et al. 2023). To leverage these markerless datasets effectively for applications in urban planning, it is essential to accurately estimate camera trajectories. This requirement arises because most online videos are captured using dynamic, moving cameras that do not provide GT camera trajectories.

Existing camera trajectory estimation techniques, including optical flow-based methods such as Droid-SLAM (Teed and Deng 2021) and DPVO (Teed, Lipson, and Deng 2023), as well as Tracking Any Point (TAP) approaches like LEAP-VO (Chen et al. 2024b), primarily rely on RGB video inputs to recover camera motion. However, their performance deteriorates in the presence of large moving objects—such as pedestrians and vehicles—that occupy significant portions of the frame. These dynamic objects can mislead the models, resulting in inaccurate trajectory estimations.

A promising strategy to mitigate this issue involves detecting and masking moving objects within the video frames during the bundle adjustment (BA) process. The primary challenge, therefore, is *how to effectively detect moving objects in videos captured by dynamic cameras*. Traditional moving object detection methods, which typically depend on background subtraction and motion detection using RGB data (Ellenfeld et al. 2021), encounter substantial difficulties in dynamic camera scenarios. These challenges include distinguishing between camera-induced motion and object motion, managing motion blur, and handling occlusions in cluttered urban environments (Yazdi and Bouwmans 2018).

To address these limitations, we propose a novel framework *MONA*, Moving Object detection from videos shot by dyNAmic Camera. Our approach comprises two main modules: *Dynamic Points Extraction* and *Moving Object Segmentation*. The *Dynamic Points Extraction* calculates the probability of selected points within the video are dynamic (moving) similar to LEAP-VO (Chen et al. 2024b). Subsequently, an optical flow-based thresholding strategy is employed to classify each point as either dynamic or static.

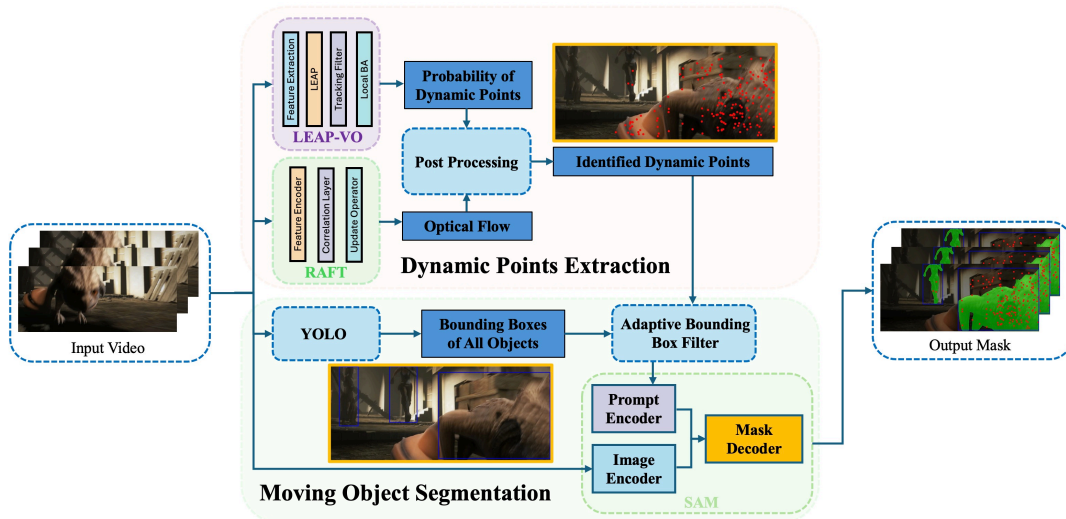


Figure 1: **The overall pipeline of *MONA*.** Our method consists of two main modules: *Dynamic Points Extraction* and *Moving Object Segmentation*. In *Dynamic Points Extraction*, random points are selected and LEAP-VO estimates the probability of each point being dynamic. RAFT then computes the optical flow, and a post-processing algorithm combines these results to identify dynamic points. In *Moving Object Segmentation*, YOLO detects all object bounding boxes, which are filtered using the dynamic points through our designed adaptive bounding box filter to identify moving objects. Finally, the filtered bounding boxes are used as prompt input to SAM to get the segmentation of the moving objects from the input video.

The *Moving Object Segmentation* leverages the identified dynamic points to segment moving objects. This is achieved by utilizing YOLO (Khanam and Hussain 2024) to detect objects in each frame and determine the bounding boxes (bboxes) that encompass the dynamic points through our proposed adaptive bbox filtering algorithm. These bboxes serve as prompt inputs to the Segment Anything Model (SAM) (Kirillov et al. 2023), which generates precise masks of the moving objects. We validate our framework through downstream tasks, such as camera trajectory estimation, demonstrating state-of-the-art (SOTA) performance on the MPI Sintel Dataset (Butler et al. 2012).

Methods

In this section, we introduce *MONA*, a framework for detecting moving objects in videos captured by dynamic cameras. The system overview is shown in Fig. 1. Given an input video sequence $V = [F_1, \dots, F_T]$, where F_t represents the frame at time t , *MONA* firstly uses *Dynamic Points Extraction* to detect all dynamic points \mathbf{X}_d based on LEAP-VO (Chen et al. 2024b), RAFT (Teed and Deng 2020) and our post-processing algorithm. Subsequently, our method uses *Moving Object Segmentation* to detect and segment all moving objects based on the input dynamic points, YOLO (Khanam and Hussain 2024), SAM (Kirillov et al. 2023) and our adaptive bounding box filter.

Dynamic Points Extraction. This module identifies dynamic points within the video. Following the approach of LEAP-VO (Chen et al. 2024b), we initially select n random detection points $\mathbf{X} = [\mathbf{x}_1, \dots, \mathbf{x}_n]$ and m anchor points from the first frame. Anchor points are chosen based on image gradients by dividing each frame F_t into $k \times k$ grids and

selecting the point with the highest gradient in each grid. We then apply the TAP method from CoTracker (Karaev et al. 2024) to obtain the trajectories a and visibility v for both detection and anchor points, shown as

$$(a, v) = \text{CoTracker}(V, \mathbf{x}_q, t_q), \quad (1)$$

where \mathbf{x}_q is the selected point and t_q is the index of the frame from which \mathbf{x}_q is extracted. The image features for each frame of the video are extracted by a CNN, and we calculate point features \mathbf{f} through bilinear sampling from the image feature map at query points \mathbf{x}_q .

Next, we compute the probability that each detection point \mathbf{x}_i is dynamic by utilizing the anchor-based pixel tracking strategy from LEAP-VO. The core idea is to compare the movement patterns of detection points with those of anchor points to infer the dynamic probability of each \mathbf{x}_i . Let $\mathbf{x} = [x, y]$ represent the pixel coordinates, where x and y are assumed to be independent. The trajectory distribution of pixel \mathbf{x} is modeled as the product of two univariate Cauchy distributions as

$$p(\mathbf{x}|V, \mathbf{x}_q) = p(x|V, \mathbf{x}_q) \cdot p(y|V, \mathbf{x}_q), \quad (2)$$

where \mathbf{x}_q is the query point. The probability density function (PDF) of coordinates can be calculated as

$$p(x|V, \mathbf{x}_q) = \frac{\left(\frac{1}{2}\right)! \left(\frac{S+1}{2} - 1\right)!}{\pi^{S/2} |\Sigma_x|^{1/2}} \times [(x - \mu_x)^\top \Sigma_x^{-1} (x - \mu_x) + 1]^{-\frac{S+1}{2}}, \quad (3)$$

where μ_x is the location matrix and Σ_x is the scale matrix respectively, the PDF of y is calculated similarly. The scale

Method	ATE (m)↓	RPE trans. (m)↓	RPE rot. (deg)↓
DROID-SLAM (Teed and Deng 2021)	0.175	0.084	1.912
Tartan VO (Wang, Hu, and Scherer 2020)	0.238	0.084	1.305
Dytan VO (Shen et al. 2023)	0.131	0.097	1.538
DPVO (Teed, Lipson, and Deng 2023)	0.076	0.078	1.722
LEAP-VO (Chen et al. 2024b)	0.068	0.035	0.150
MONA+ LEAP-VO (Ours)	0.029	0.013	0.054

Table 1: **Comparison of the performance between methods on MPI Sintel Dataset.** Compared to the original LEAP-VO, our proposed method (*MONA+ LEAP-VO*) has achieved over 60% improvement on ATE, RPE trans. and RPE rot., demonstrating that *MONA*’s performance on moving object detection and its effectiveness of *MONA* in camera trajectory estimation tasks.

matrices Σ_x and Σ_y are constructed by kernel-based estimation to ensure they are symmetric and positive definite, we apply a linear kernel to projected point features and add regularization, as shown in Eq. 4.

$$\Sigma_x = \mathbf{f}_x^\top \mathbf{f}_x + \lambda I \quad (4)$$

λI is the regularization term. The Σ_y can be calculated using similar procedure shown in Eq. 4.

After obtaining the dynamic probability p for each point \mathbf{x} , a threshold is required to classify points as dynamic or static. Manually setting a fixed threshold is suboptimal due to varying camera movements across different frames within the same video. To address this, we propose a post-processing step that dynamically determines the threshold for each frame by integrating optical flow information. Specifically, we compute the optical flow $\mathbf{u}_t(\mathbf{x})$ for each pixel using RAFT (Teed and Deng 2020) and calculate the mean magnitude \bar{m}_t for frame F_t . This adaptive thresholding approach ensures more accurate identification of dynamic points by accounting for the specific motion characteristics of each frame. The \bar{m}_t is calculated as

$$\bar{m}_t = \frac{1}{|\Omega|} \sum_{\mathbf{x} \in \Omega} \|\mathbf{u}_t(\mathbf{x})\|, \quad (5)$$

where Ω denotes the set of all points (pixels) in the frame and $|\Omega|$ represents the total number of points. Using the mean magnitude \bar{m}_t , we dynamically scale the threshold θ_t for identifying dynamic points in frame t . Detection points \mathbf{x} in frame t with magnitudes exceeding θ_t are classified into the dynamic points list \mathbf{x}_d and will input to *Moving Object Segmentation* for the segmentation of moving objects.

Moving Object Segmentation. To segment moving objects from the dynamic points list \mathbf{x}_d , objects in each frame are first detected using YOLO, resulting in bounding boxes $\mathcal{B} = b_1, \dots, b_n$. Since YOLO cannot differentiate between static and dynamic objects, an adaptive bounding box filter is applied using \mathbf{x}_d and \mathcal{B} to exclude bounding boxes b_i corresponding to static objects. Let D_i denote the number of dynamic points within bounding box b_i . Manually setting a threshold based on D_i may inadvertently classify larger bounding boxes as moving objects. To ensure consistency across varying bounding box sizes, a threshold τ_0 is established for moving objects within the video. The smallest bounding box b_u in \mathcal{B} where D_u exceeds τ_0 is identified,

and its area is used as the unit area. Subsequently, the threshold τ_t^i for each bounding box b_i in frame t is scaled based on the ratio of the area of b_i to that of b_u , shown as

$$\tau_t^i = \tau_0 \times \frac{\text{Area}(b_i)}{\text{Area}(b_u)}, u = \arg \min_{b \in \mathcal{B}} \{\text{Area}(b) \mid D_u \geq \tau_0\} \quad (6)$$

The filtered bounding boxes are defined as $\mathcal{B}_{\text{filtered}} = \{b_i \mid D_i \geq \tau_t^i, b_i \in \mathcal{B}\}$, which determine whether the bounding boxes belong to truly moving objects. $\mathcal{B}_{\text{filtered}}$ denotes high-quality prompts to SAM for segmentation.

Experiments and Results

Currently, no public dataset is available to directly evaluate detection accuracy and mask quality for moving objects in videos captured by moving cameras. Therefore, we selected camera trajectory estimation as our downstream testing task, based on the hypothesis that accurately detecting and masking moving objects enhances camera trajectory estimation. By masking dynamic objects, the model can focus on static regions, improving the selection of tracked points and reducing noise from moving entities. For this purpose, we integrate our method with LEAP-VO (Chen et al. 2024b), a camera trajectory estimation method, to evaluate *MONA*’s performance for moving object detection by analyzing the output estimated camera trajectory of *MONA+LEAP-VO*.

For an initial qualitative evaluation, we compared the original LEAP-VO, *MONA+LEAP-VO*, and the ground truth trajectories using raw videos from the MPI Sintel dataset (Butler et al. 2012). Figure 2 shows two selected examples, demonstrating that our method significantly enhances trajectory estimation. By accurately detecting and masking moving objects during bundle adjustment in LEAP-VO, *MONA+LEAP-VO* produces camera trajectories that closely match the ground truth, regardless of the complexity of the camera motion. These results highlight the robustness and adaptability of our approach across various scenarios.

To quantitatively evaluate our proposed method, we compared the original LEAP-VO with *MONA+LEAP-VO* on the MPI Sintel dataset (Butler et al. 2012) for camera trajectory estimation. As shown in Table 1, we assessed performance using three metrics: Absolute Trajectory Error (ATE), Relative Translation Error (RPE trans), and Relative Rotation Error (RPE rot). *MONA+LEAP-VO* achieved over a 60% improvement across all metrics, significantly outperforming

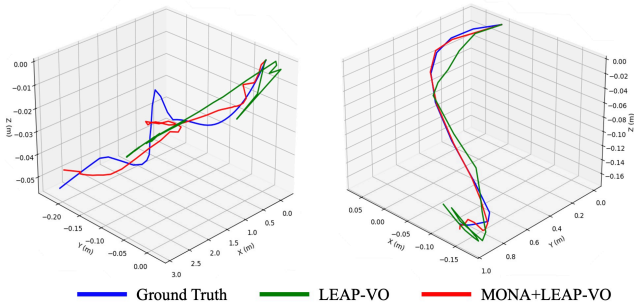


Figure 2: **Qualitative Comparison on Estimated Camera Trajectory between different methods.** We run original LEAP-VO and LEAP-VO with *MONA* on MPI Sintel Dataset (Butler et al. 2012). Two estimated trajectories are selected as the comparison. The *MONA+LEAP-VO* provides a more accurate estimated trajectory as it is more similar to the GT, which demonstrates the effectiveness of our method in camera trajectory estimation tasks.

existing SOTA methods. These results validate the effectiveness of our approach in enhancing trajectory estimation accuracy, particularly in scenarios with moving objects.

The substantial improvements of *MONA+LEAP-VO* in camera trajectory estimation are due to its enhanced selection of tracked points in the TAP pipeline through moving object detection and segmentation. While LEAP-VO initially selects random points and filters dynamic ones by comparing them to anchor points, this approach does not consistently avoid dynamic object regions due to the difficulty in determining optimal thresholds. By incorporating *MONA*, it can address this limitation by first detecting all moving objects and getting their masks. Then, the randomly selected points inside the moving objects mask can be filtered in the bundle adjustment process in LEAP-VO, thereby improving the quality of output estimated camera trajectory.

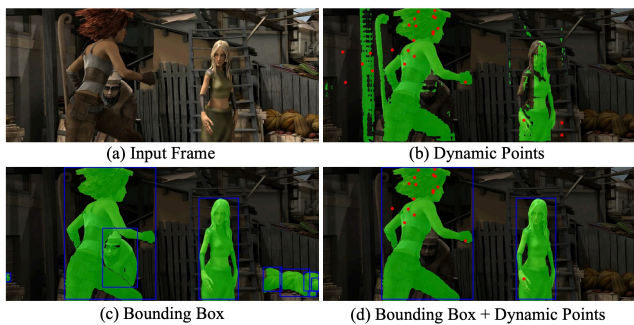


Figure 3: **Qualitative Ablation Study of *MONA*.** We visualize and compare the quality of masks produced by different prompts input to SAM: (b) pure dynamic points (c) pure bounding boxes (without filtering), and (d) bounding boxes with dynamic points filtering strategy.

Ablation Study. We compared the segmentation results produced by three approaches: using only dynamic points as prompts, using YOLO’s raw bounding boxes, and using our

filtered bounding boxes. The visualization of Fig. 3 visualizes these results. Using only dynamic points as prompts resulted in incomplete masks and incorrect segmentations (Fig. 3 (b)), while YOLO’s raw bounding boxes failed to distinguish between static and dynamic objects ((Fig. 3 (c))). In contrast, our pipeline, which incorporates filtered bounding boxes, consistently produced accurate and effective segmentation masks for moving objects (Fig. 3 (d)). These findings demonstrate the superiority of our approach in accurately detecting moving objects and generating high-quality masks, which are essential for improving the performance of downstream tasks like camera trajectory estimation.

Conclusion

In this paper, we introduce *MONA*, a robust framework for detecting moving objects in RGB videos captured by dynamic cameras. Our method effectively separates camera-induced motion from object motion in in-the-wild footage. *MONA* enhances various tasks, particularly camera trajectory estimation, by complementing existing approaches. When integrated with LEAP-VO, *MONA* achieves state-of-the-art performance on the MPI Sintel Dataset. Given that an accurate camera trajectory estimation is essential for creating markerless datasets used in ADS, UAV motion planning, and HMR, *MONA* offers new opportunities in both datasets and other applications in the urban planning domain.

References

- Bescos, B.; Facil, J. M.; Civera, J.; and Neira, J. 2018. DynaSLAM: Tracking, Mapping, and inpainting in Dynamic Scenes. *IEEE Robotics and Automation Letters*, 3(4): 4076–4083.
- Butler, D. J.; Wulff, J.; Stanley, G. B.; and Black, M. J. 2012. A naturalistic open source movie for optical flow evaluation. In A. Fitzgibbon et al. (Eds.), ed., *European Conf. on Computer Vision (ECCV)*, Part IV, LNCS 7577, 611–625. Springer-Verlag.
- Caldeira, J.; Fout, A.; Kesari, A.; Sefala, R.; Walsh, J.; Dupre, K.; Khaefi, M. R.; Setiaji; Hodge, G.; Pramestri, Z. A.; et al. 2020. Improving traffic safety through video analysis in Jakarta, Indonesia. In *Intelligent Systems and Applications: Proceedings of the 2019 Intelligent Systems Conference (IntelliSys) Volume 2*, 642–649. Springer.
- Chapel, M.-N.; and Bouwmans, T. 2020. Moving objects detection with a moving camera: A comprehensive review. *Computer science review*, 38: 100310.
- Chen, L.-H.; Lu, S.; Zeng, A.; Zhang, H.; Wang, B.; Zhang, R.; and Zhang, L. 2024a. MotionLLM: Understanding Human Behaviors from Human Motions and Videos. *arXiv preprint arXiv:2405.20340*.
- Chen, W.; Chen, L.; Wang, R.; and Pollefeys, M. 2024b. LEAP-VO: Long-term Effective Any Point Tracking for Visual Odometry. In *CVPR*.
- Chen, X.; Ma, H.; Wan, J.; Li, B.; and Xia, T. 2017. Multi-view 3D Object Detection Network for Autonomous Driving. In *2017 IEEE Conference on Computer Vision and Pattern Recognition (CVPR)*, 6526–6534.

- Chen, Y.; Liu, S.; Shen, X.; and Jia, J. 2019. Fast Point R-CNN. In *2019 IEEE/CVF International Conference on Computer Vision (ICCV)*, 9774–9783.
- Ellenfeld, M.; Moosbauer, S.; Cardenes, R.; Klauck, U.; and Teutsch, M. 2021. Deep fusion of appearance and frame differencing for motion segmentation. In *proceedings of the IEEE/CVF Conference on Computer Vision and Pattern Recognition*, 4339–4349.
- Foth, M.; Heikkinen, T.; Ylipulli, J.; Luusua, A.; Satchell, C.; and Ojala, T. 2014. UbiOpticon: participatory sousveillance with urban screens and mobile phone cameras. In *Proceedings of The International Symposium on Pervasive Displays*, 56–61.
- Guo, C.; Zuo, X.; Wang, S.; and Cheng, L. 2022. Tm2t: Stochastic and tokenized modeling for the reciprocal generation of 3d human motions and texts. In *ECCV*, 580–597.
- Huang, C.; Fang, S.; Wu, H.; Wang, Y.; and Yang, Y. 2024. Low-altitude intelligent transportation: System architecture, infrastructure, and key technologies. *Journal of Industrial Information Integration*, 42: 100694.
- Jiang, B.; Chen, X.; Liu, W.; Yu, J.; Yu, G.; and Chen, T. 2024. Motiongpt: Human motion as a foreign language. *NeurIPS*.
- Karaev, N.; Rocco, I.; Graham, B.; Neverova, N.; Vedaldi, A.; and Ruppel, C. 2024. CoTracker: It is Better to Track Together. In *Proc. ECCV*.
- Karagulyan, F.; Libertino, C.; Corazza, M.; Valenti, G.; Dumitru, A.; and Nigro, M. 2023. Pedestrian flows characterization and estimation with computer vision techniques. *Urban Science*, 7(2): 65.
- Khanam, R.; and Hussain, M. 2024. Yolov11: An overview of the key architectural enhancements. *arXiv preprint arXiv:2410.17725*.
- Kirillov, A.; Mintun, E.; Ravi, N.; Mao, H.; Rolland, C.; Gustafson, L.; Xiao, T.; Whitehead, S.; Berg, A. C.; Lo, W.-Y.; et al. 2023. Segment anything. In *Proceedings of the IEEE/CVF International Conference on Computer Vision*, 4015–4026.
- Ku, J.; Mozifian, M.; Lee, J.; Harakeh, A.; and Waslander, S. L. 2018. Joint 3D Proposal Generation and Object Detection from View Aggregation. In *2018 IEEE/RSJ International Conference on Intelligent Robots and Systems (IROS)*, 1–8.
- Lang, A. H.; Vora, S.; Caesar, H.; Zhou, L.; Yang, J.; and Beijbom, O. 2019. PointPillars: Fast Encoders for Object Detection From Point Clouds. In *2019 IEEE/CVF Conference on Computer Vision and Pattern Recognition (CVPR)*, 12689–12697.
- Li, B. 2017. 3D fully convolutional network for vehicle detection in point cloud. In *2017 IEEE/RSJ International Conference on Intelligent Robots and Systems (IROS)*, 1513–1518.
- Li, B.; Ouyang, W.; Sheng, L.; Zeng, X.; and Wang, X. 2019. GS3D: An Efficient 3D Object Detection Framework for Autonomous Driving. 1019–1028.
- Li, Z.; Gao, Z.; Wang, K.; Mei, Y.; Zhu, C.; Chen, L.; Wu, X.; and Niyato, D. 2024. Unauthorized UAV Countermeasure for Low-Altitude Economy: Joint Communications and Jamming Based on MIMO Cellular Systems. *IEEE Internet of Things Journal*, 1–1.
- Lin, J.; Zeng, A.; Lu, S.; Cai, Y.; Zhang, R.; Wang, H.; and Zhang, L. 2023. Motion-X: A Large-scale 3D Expressive Whole-body Human Motion Dataset. *Advances in Neural Information Processing Systems*.
- Moon, G.; Choi, H.; and Lee, K. M. 2022. NeuralAnnot: Neural Annotator for 3D Human Mesh Training Sets. In *Computer Vision and Pattern Recognition Workshop (CVPRW)*.
- Mur-Artal, M. J. M. M., Raúl; and Tardós, J. D. 2015. ORB-SLAM: a Versatile and Accurate Monocular SLAM System. *IEEE Transactions on Robotics*, 31(5): 1147–1163.
- Myagmar-Ochir, Y.; and Kim, W. 2023. A survey of video surveillance systems in smart city. *Electronics*, 12(17): 3567.
- Nikolakakis, N.; Maratos, V.; and Makris, S. 2019. A cyber physical system (CPS) approach for safe human-robot collaboration in a shared workplace. *Robotics and Computer-Integrated Manufacturing*, 56: 233–243.
- Pang, H. E.; Cai, Z.; Yang, L.; Zhang, T.; and Liu, Z. 2024. Benchmarking and analyzing 3D human pose and shape estimation beyond algorithms. In *Proceedings of the 36th International Conference on Neural Information Processing Systems, NIPS '22*. Red Hook, NY, USA: Curran Associates Inc. ISBN 9781713871088.
- Shen, S.; Cai, Y.; Wang, W.; and Scherer, S. 2023. DytanVO: Joint Refinement of Visual Odometry and Motion Segmentation in Dynamic Environments. In *2023 IEEE International Conference on Robotics and Automation (ICRA)*, 4048–4055.
- Shen, Z.; Pi, H.; Xia, Y.; Cen, Z.; Peng, S.; Hu, Z.; Bao, H.; Hu, R.; and Zhou, X. 2024. World-Grounded Human Motion Recovery via Gravity-View Coordinates. In *ACM SIGGRAPH Asia*.
- Shi, S.; Wang, X.; and Li, H. 2019. PointRCNN: 3D Object Proposal Generation and Detection From Point Cloud. In *The IEEE Conference on Computer Vision and Pattern Recognition (CVPR)*.
- Shi, S.; Wang, Z.; Shi, J.; Wang, X.; and Li, H. 2019. From Points to Parts: 3D Object Detection from Point Cloud with Part-aware and Part-aggregation Network. *arXiv preprint arXiv:1907.03670*.
- Shin, S.; Kim, J.; Halilaj, E.; and Black, M. J. 2024. WHAM: Reconstructing World-grounded Humans with Accurate 3D Motion. In *CVPR*.
- Teed, Z.; and Deng, J. 2020. Raft: Recurrent all-pairs field transforms for optical flow. In *Computer Vision—ECCV 2020: 16th European Conference, Glasgow, UK, August 23–28, 2020, Proceedings, Part II 16*, 402–419. Springer.
- Teed, Z.; and Deng, J. 2021. DROID-SLAM: Deep Visual SLAM for Monocular, Stereo, and RGB-D Cameras. In *Ranzato, M.; Beygelzimer, A.; Dauphin, Y.; Liang, P.; and*

Vaughan, J. W., eds., *NeurIPS*, volume 34, 16558–16569. Curran Associates, Inc.

Teed, Z.; Lipson, L.; and Deng, J. 2023. Deep Patch Visual Odometry. *NeurIPS*.

Tordesillas, J.; and How, J. P. 2023. Deep-PANTHER: Learning-Based Perception-Aware Trajectory Planner in Dynamic Environments. *IEEE Robotics and Automation Letters*, 8(3): 1399–1406.

Wang, J.; Yuan, Y.; Luo, Z.; Xie, K.; Lin, D.; Iqbal, U.; Fidler, S.; and Khamis, S. 2023. Learning Human Dynamics in Autonomous Driving Scenarios. In *ICCV*, 20739–20749.

Wang, W.; Hu, Y.; and Scherer, S. 2020. TartanVO: A Generalizable Learning-based VO.

Wang, W.; Li, R.; Chen, Y.; Diekel, Z. M.; and Jia, Y. 2019. Facilitating Human–Robot Collaborative Tasks by Teaching-Learning-Collaboration From Human Demonstrations. *IEEE Transactions on Automation Science and Engineering*, 16(2): 640–653.

Wu, G.; Zhao, Z.; and He, Y. 2024. RELAX: Reinforcement Learning Enabled 2D-LiDAR Autonomous System for Parsimonious UAVs. arXiv:2309.08095.

Xiong, K.; Xie, J.; and Leng, S. 2024. eVTOL Communication and Trajectory Optimization in Low-Altitude Economy. In *2024 IEEE/CIC International Conference on Communications in China (ICCC Workshops)*, 845–850.

Yazdi, M.; and Bouwmans, T. 2018. New trends on moving object detection in video images captured by a moving camera: A survey. *Computer science review*, 28: 157–177.

Ye, V.; Pavlakos, G.; Malik, J.; and Kanazawa, A. 2023. Decoupling Human and Camera Motion from Videos in the Wild. In *CVPR*.

Yuan, Y.; Iqbal, U.; Molchanov, P.; Kitani, K.; and Kautz, J. 2022. Glamr: Global occlusion-aware human mesh recovery with dynamic cameras. In *Proceedings of the IEEE/CVF conference on computer vision and pattern recognition*, 11038–11049.

Zhou, B.; Pan, J.; Gao, F.; and Shen, S. 2021. RAPTOR: Robust and Perception-Aware Trajectory Replanning for Quadrotor Fast Flight. *IEEE Transactions on Robotics*, 37(6): 1992–2009.